Radiative $\Upsilon(1S)$ decays

R. Fulton, M. Hempstead, T. Jensen, D. R. Johnson, H. Kagan, R. Kass, F. Morrow, and J. Whitmore
Ohio State University, Columbus, Ohio 43210

W.-Y. Chen, J. Dominick, R. L. McIlwain, D. H. Miller, C. R. Ng, E. I. Shibata, and W.-M. Yao
Purdue University, West Lafayette, Indiana 47907

K. Sparks and E. H. Thorndike
University of Rochester, Rochester, New York 14627

M. S. Alam, N. Katayama, I. J. Kim, W. C. Li, X. C. Lou, and C. R. Sun
State University of New York at Albany, Albany, New York 12222

D. Bortoletto, M. Goldberg, N. Horwitz, P. Lubrano, M. D. Mestayer, G. C. Moneti, V. Sharma, I. P. J. Shipsey, and T. Skwarnicki
Syracuse University, Syracuse, New York 13244

S. E. Csorna and T. Letson
Vanderbilt University, Nashville, Tennessee 37235

I. C. Brock, T. Ferguson, and H. Vogel
Carnegie Mellon University, Pittsburgh, Pennsylvania 15213

J. Alexander, M. Artuso, C. Bebek, J. Byrd, K. Berkelman, E. Blucher, D. G. Cassel, E. Cheu, D. M. Coffman, T. Copie, G. Crawford, J. W. DeWire, P. S. Drell, R. Ehrlich, R. S. Galik, B. Gittelman, S. W. Gray, A. M. Halling, D. L. Hartill, B. K. Heltsley, J. Kandaswamy, R. Kowalewski, D. L. Kreinick, Y. Kubota, J. D. Lewis, N. B. Mistry, J. Mueller, R. Namjoshi, S. Nandi, E. Nordberg, C. O'Grady, D. Peterson, M. Pisharody, D. Riley, M. Sapper, A. Silverman, S. Stone, H. Worden, and M. Worris
Cornell University, Ithaca, New York 14853

A. J. Sadoff
Ithaca College, Ithaca, New York 14850

P. Avery, D. Besson, L. Garren, and J. Yelton
University of Florida, Gainesville, Florida 32611

T. Bowcock, K. Kinoshita, F. M. Pipkin, M. Procario, Richard Wilson, J. Wolinski, and D. Xiao
Harvard University, Cambridge, Massachusetts 02138

P. Baringer, P. Haas, and Ha Lam
University of Kansas, Lawrence, Kansas 66045

A. Jawahery and C. H. Park
University of Maryland, College Park, Maryland 20742

D. Perticone and R. Poling
University of Minnesota, Minneapolis, Minnesota 55455
(Received 5 May 1989)

We report on a study of exclusive radiative decays of the $\Upsilon(1S)$ resonance. We have considered decays into final states of the form $\Upsilon \to \gamma n(h^+h^-)$, with (h^+h^-) denoting a charged-hadron pair (either $\pi^+\pi^-$, K^+K^-, or $p\bar{p}$), and n denoting the number of such pairs in the event. We measure branching ratios for $n=2$, 3, and 4, and search for structure in the recoiling hadronic system. For the $n=1$ case, we present upper limits. No evidence is observed for two-body radiative decays of the $\Upsilon(1S)$ meson in any of the above channels.

I. INTRODUCTION

A particularly interesting class of $\Upsilon(1S)$ decays are the radiative decays, which could show evidence for the same type of two-body decays as have been observed in ψ decay.[1] Simple scaling arguments estimate suppressions of order $[(q_b/q_c)(m_c/m_b)]^2$ in the relative branching ratios for such decays between the $\Upsilon(1S)$ and the ψ; more sophisticated calculations can be found in the literature.[2] In particular, if the recoil state is a pseudoscalar glueball instead of a conventional hadronic state, the mass suppression may vary as a power of 6 rather than 2.[2] We have conducted a search for such exclusive radiative decays of the $\Upsilon(1S)$ using the CLEO detector at the Cornell Electron Storage Ring (CESR).

The data sample consists of 15.5 pb^{-1} of $\Upsilon(1S)$ data collected with the initial form of the CLEO detector, and 21.0 pb^{-1} of $\Upsilon(1S)$ data collected with the recently improved CLEO detector. The full data sample corresponds to 825 000 $\Upsilon(1S)$ decays and 150 000 hadronic-continuum e^+e^- annihilation events under the resonance. We use a sample of 101 pb^{-1} collected on the continuum below the $\Upsilon(4S)$ for background studies (corresponding to 380 000 hadronic-continuum events).

The CLEO detector in its initial configuration has been described in detail elsewhere;[3] here we will briefly describe the recent modifications to the central tracking system. Charged-particle tracking is performed inside a superconducting solenoid of radius 1.0 m which produces a 1.0-T magnetic field. Three nested cylindrical drift chambers measure momenta and specific ionization for charged particles. The innermost part of the tracking system is a three-layer straw tube vertex detector which gives position accuracy of 70 μm in the r-ϕ plane. The middle ten-layer vertex chamber measures position with an accuracy of 90 μm in the r-ϕ plane and specific ionization (dE/dx) to 14%. The main drift-chamber system[4] contains 51 layers, 11 of which are strung at stereo angles of 1.9° to 3.5° to the z axis, providing an r-ϕ position accuracy of 110 μm and dE/dx to 6.5%. Measurements of the track coordinates along the beam position (z) are achieved by using the stereo layers and cathode-strip readouts in the middle vertex detector and the main drift chamber. The system achieves a momentum resolution given by $(\delta p/p)^2=(0.23\%p)^2+(0.7\%)^2$, where p is in GeV/c. For all the data used in these analyses, photon detection is performed with the barrel electromagnetic calorimeters, which cover 47% of the solid angle and give an energy resolution $\sigma_E/E=21\%/\sqrt{E(\text{GeV})}$. The angular resolution of the calorimeter is approximately 10 mrad.

II. EVENT SELECTION

We search for events satisfying the kinematics of the processes $\Upsilon\to\gamma n(h^+h^-)$ using the following criteria.

(a) The net charge (q_{tot}) of the tracks observed in the drift chamber is required to be zero.

(b) There must exist at least one electromagnetic shower observed in the barrel calorimeter which does not match (within 0.1 rad) the position of any charged track extrapolated beyond the drift chamber into the barrel calorimeter.

(c) None of the charged tracks in the event are identified as leptons.[5]

(d) The sum of the observed photon energy plus the energies of the drift-chamber tracks (allowing for all possible permutations of $\pi^+\pi^-$, K^+K^-, and $p\bar{p}$ pairs) must, under at least one event-type hypothesis, lie within three standard deviations (taking into account photon energy and track momentum resolutions) of the total center-of-mass energy.

(e) For $n=1$ candidates, we require that the opening angle ϕ between the two tracks satisfy the condition $\cos\phi>-0.5$. This condition, previously employed in a similar analysis,[6] is very effective at removing QED backgrounds, where two leptons often emerge approximately anticollinear from the interaction point.

We also collect events satisfying criteria (b), (c), and (d), but with $|q_{\text{tot}}|=1$ for the purposes of doing background studies.

III. ANALYSIS AND RESULTS: $\Upsilon\to\gamma n(h^+h^-)$, $n>1$

For $n>1$ candidate events, we define p_h as the magnitude of the net momentum of the charged tracks. In real $\Upsilon\to\gamma n(h^+h^-)$ decays, the energy of the photon must equal p_h, and the angle θ between the photon direction and the direction of the net charged momentum vector $\mathbf{p}_h$ must be 180°. Defining $\delta_p=(E_\gamma-p_h)/\sigma_E$ as the deviation between the energy of the observed photon (E_γ) and the net momentum of the charged tracks in units of the resolution σ_E of the electromagnetic calorimeter, we plot δ_p vs $\cos\theta$. Event candidates are expected to populate the region near $\cos\theta=-1.0$ and $\delta_p=0.0$. The plot for the case $n=2$ is shown in Fig. 1.

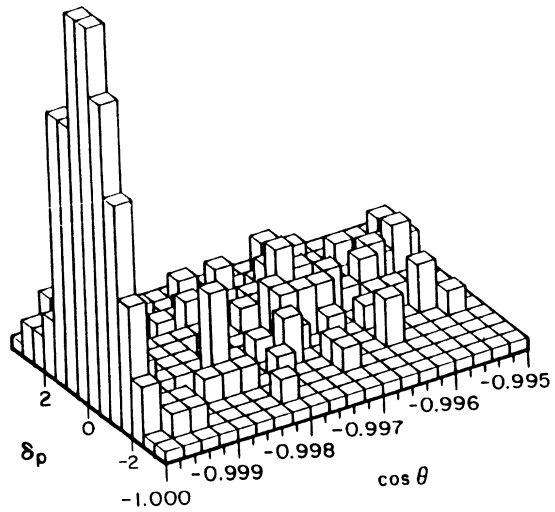

FIG. 1. Number of observed $\Upsilon\to\gamma 2(h^+h^-)$ events as a function of $\cos\theta$ and δ_p, where $\cos\theta$ is the cosine of the opening angle between the charged-particle net momentum and the photon direction, and δ_p is the difference between the photon momentum and the charged-particle momentum normalized to the detector resolution. The peak bin contains 16 events.

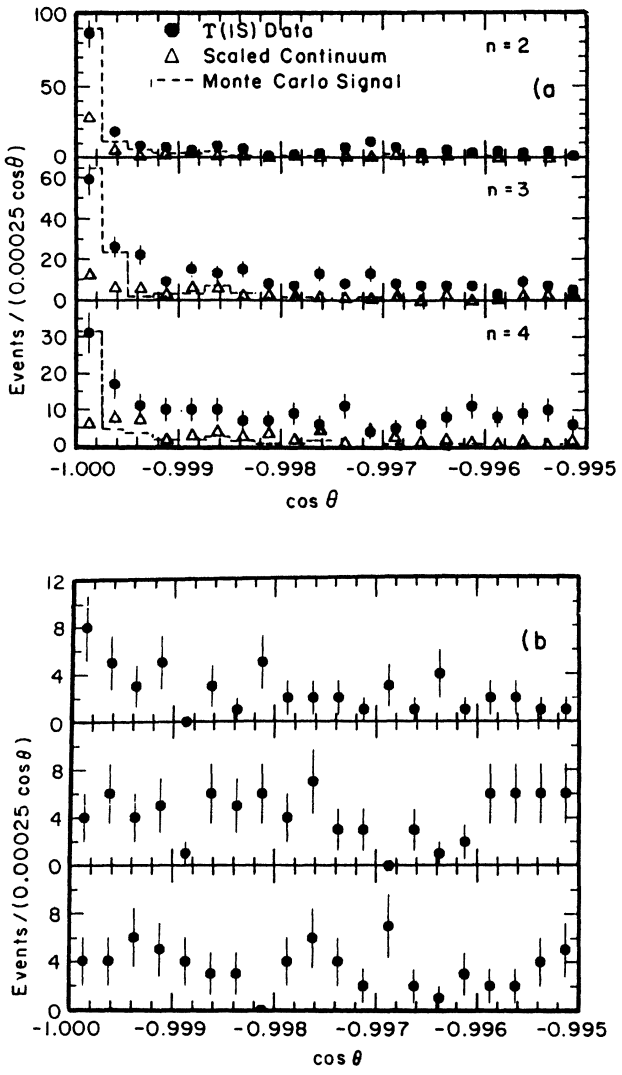

FIG. 2. (a) Projections onto $\cos\theta$ axis for $n=2$, 3, and 4; and (b) projections obtained for events with total charge of magnitude 1.

By selecting the band with $|\delta_p|<2.0$ and projecting onto the $\cos\theta$ axis, we obtain Fig. 2(a). Overplotted are the projections obtained using continuum (open triangles), and the signal shape expected from $\Upsilon\to\gamma n(h^+h^-)$ Monte Carlo events (dashed line) arbitrarily normalized to data. The continuum data have been scaled for luminosity and energy differences in order to correspond to the nonresonant portion of the data taken at the $\Upsilon(1S)$ energy. Also shown are the projections obtained by carrying out this procedure for the cases $n=2$, 3, and 4. Extrapolating a linear background from the region $\cos\theta\geq-0.9995$ into the two leftmost bins on these plots (corresponding to the region $\cos\theta\leq-0.9995$), we observe clear evidence for an excess for the cases $n=2$, 3, and 4 (in all that follows, we will consider as our signal events those events above the flat background in the interval $\cos\theta\leq-0.9995$ and $|\delta_p|<2.0$). In Fig. 2(b), we show the projections we obtain using $|q_{\rm tot}|=1$ events; these are considered to be representative of the shape of the background which arises from events where there is at least one undetected particle in the event. We note that the total charge-one events give spectra which are not peaked in the signal region.

In order to establish how many of the signal events for $n=2$, 3, and 4 are due to radiative $\Upsilon(1S)$ decays, we study possible background sources and subtract their contributions. The numbers of signal and background events are summarized in Tables I–III.

One possible background source of $\gamma+$hadrons is the continuum process $e^+e^-\to q\bar{q}\gamma$, in which the photon is emitted from one of the incident leptons. We have verified that our continuum data near $\cos\theta=-1.0$ are numerically consistent with this process by using a Monte Carlo program with QED corrections[7] to generate continuum e^+e^- events. From this study, we predict 34 ± 8 such events in the $n=2$ continuum data sample for the region $\cos\theta\leq-0.9995$, whereas we actually observe an excess of 27 ± 6 events in the continuum data above background.

We have attempted to establish whether an observed

TABLE I. Summary of T_2 and of $\Upsilon\to\gamma2(h^+h^-)$ analysis.

	Generated Y			
	$Y_1=4\pi$	$Y_2=2\pi2K$	$Y_3=2\pi2p$	$Y_4=4K$
Observed $X_1=4\pi$	0.104	0.016	0.001	0.001
Observed $X_2=2\pi2K$	0.014	0.084	0.030	0.019
Observed $X_3=2\pi2p$	0.006	0.027	0.098	0.014
Observed $X_4=4K$	0.001	0.001	0.001	0.091
Net Y efficiency	0.124	0.127	0.129	0.125

Decay mode	$X=4\pi$	$X=2\pi2K$	$X=2\pi2p$	$X=4K$	Sum $n=2$
Observed events	41±6	38±6	28±5	3±1	110±8
Continuum events	14±4	8±3	4±2	1±1	27±6
Other background	1±1	1±1	2±2	0±1	4±3
Net excess	26±7	29±8	22±6	2±2	80±12
Calculated branching ratio (10^{-4})	2.5±0.7±0.5	2.9±0.7±0.6	1.5±0.5±0.3	0.2±0.2	7.0±1.1±1.0
LUND-model branching ratio (10^{-4})					5.9±0.9

TABLE II. Summary of T_3 and of $\Upsilon \to \gamma 3(h^+h^-)$ analysis.

	Generated Y		
	$Y_1 = 6\pi$	$Y_2 = 4\pi 2K$	$Y_3 = 4\pi 2p$
Observed $X_1 = 6\pi$	0.064	0.010	0.000
Observed $X_2 = 4\pi 2K$	0.014	0.066	0.015
Observed $X_3 = 4\pi 2p$	0.003	0.013	0.077
Net Y efficiency	0.082	0.089	0.092

Decay mode	$X = 6\pi$	$X = 4\pi 2K$	$X = 4\pi 2p$	Sum $n = 3$
Observed events	23±5	29±6	27±6	79±9
Continuum events	4±2	4±2	7±3	15±5
Other background	2±1	7±3	14±4	23±6
Net excess	17±5	18±7	7±6	39±11
Calculated branching ratio (10^{-4})	2.5±0.9±0.8	2.4±0.9±0.8	0.4±0.4±0.4	5.4±1.5±1.3
LUND-model branching ratio (10^{-4})				6.9±0.9

shower is due to one photon or two overlapping photons by determining the energy-weighted spread[8] of each shower. We find, as shown in Fig. 3, that the average value of this parameter for Monte Carlo–produced merged photons from π^0 decay is well separated from the values obtained for photons from true radiative Bhabha events and photons from our candidate exclusive $\Upsilon(1S)$ decay sample.[9] The distribution in this shower-width parameter favors the single-photon interpretation for our exclusive radiative decay event candidates.

In addition, by generating 825 000 LUND (Ref. 10) Monte Carlo events of the type $\Upsilon(1S) \to ggg$, we have attempted to quantify the background due to merged photons from decays of π^0's produced in three-gluon fragmentation. For each π^0 which falls within our geometric acceptance, we use an energy-dependent probability that the π^0 will appear as a single shower[11] [obtained from EGS (Ref. 12) Monte Carlo photon showers] in our calorimeter, and we thereby derive the background to the signal $\Upsilon \to \gamma n(h^+h^-)$ from decays $\Upsilon \to \pi^0 n(h^+h^-)$. Figure 4 depicts the observed photon energy spectrum for our event candidates ($n = 2$), with the backgrounds due to continuum and $\Upsilon \to \pi^0 2(h^+h^-)$ overplotted. The background expected from the last source is less than seven events.

Finally, we have considered the possibility that asymmetric π^0 decays, which produce one high-energy photon and one soft photon, are contaminating our signal. In such a case, we expect the mean of the δ_p distribution to be shifted off center (to negative values), since the high-energy photon will always have less than the expected energy. Figure 5 shows that the observed δ_p distribution for our signal candidates fits well to a Gaussian with zero mean and unit width, as expected for a true signal. Using Monte Carlo simulations, we quantitatively estimate the contamination to the $n = 2$ signal from this source as less than three events.

We use a Monte Carlo simulation to determine the efficiency for reconstructing a radiative $\Upsilon(1S)$ event. The LUND Monte Carlo program, after being tuned to give a photon spectrum which matches experimental measurements of the photon spectrum from the $\Upsilon(1S)$,[13] is used to simulate fragmentation of the recoil gluons. The net efficiency for observing our signal is obtained by using a detector simulation to determine geometric and tracking efficiencies. We use these efficiencies to calculate the branching ratios for these modes.

TABLE III. Summary of $\Upsilon \to \gamma 4(h^+h^-)$ analysis.

Observed signal size	73±9
Continuum background	7±3
Other background	30±6
Signal (background subtracted)	36±12
Efficiency ($\Upsilon \to \gamma 4(h^+h^-)$)	0.069
Topological branching ratio (10^{-4})	7.4±2.5±2.5
LUND predicted branching ratio (10^{-4})	9.0±1.3

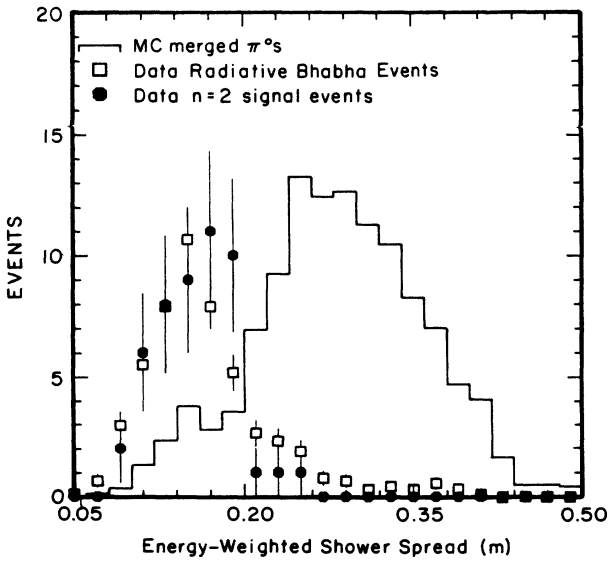

FIG. 3. Lateral spread of showers in electromagnetic calorimeter for single photons and merged π^0's.

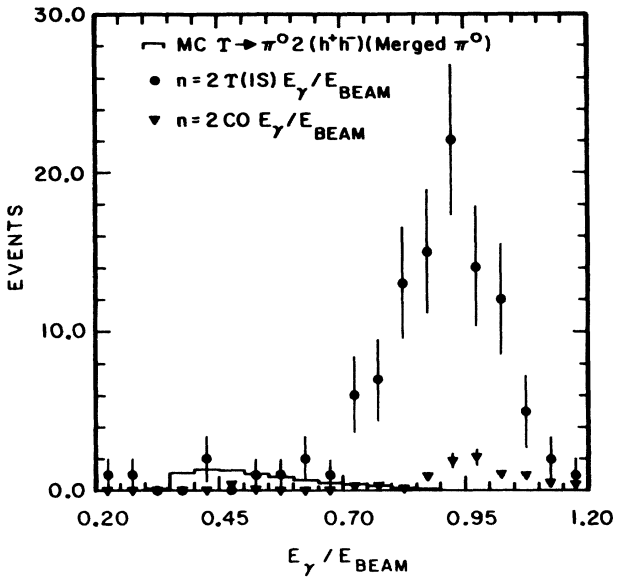

FIG. 4. Energy spectrum (normalized to beam energy) for $\Upsilon\to\gamma 2(h^+h^-)$ event candidates, with continuum data and expected background from $\Upsilon\to\pi^0 2(h^+h^-)$ overplotted.

To determine the charged-particle types recoiling against the photon, we use the particle identification capabilities of the main drift chamber in conjunction with an energy-conservation criterion to differentiate between particle hypotheses. We select the most likely charged-particle assignment for each event in the following manner: We require that oppositely signed particles, taken pairwise, both have dE/dx pulse-height depositions in the inner drift chamber which are within $\pm 2.5\sigma_{dE/dx}$ of the assumed particle identities (either $\pi^+\pi^-$, K^+K^-, or $p\bar{p}$). We then calculate, for $n=2$ and 3 events, the difference between the known event energy and the sum of the measured photon energy and the charged-particle energies under the particular combination of charged-particle mass assumptions. We retain as the most likely particle mass assignments the hypothesis which best approximates energy conservation. The number of possible event types becomes prohibitively large for the $n=4$ case and in this instance, we drop the identification requirement and consider only the simplest case with all particles considered to be pions.

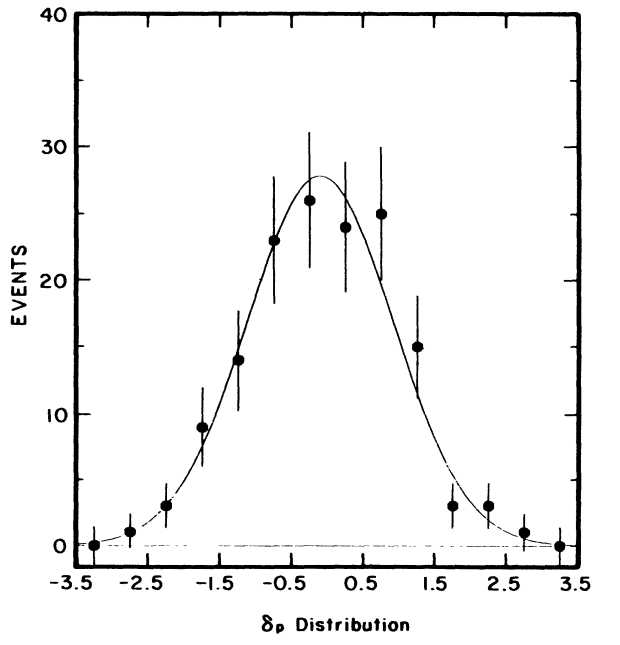

FIG. 5. Fit to δ_p distribution for sum of observed $n=2$ and $n=3$ signals.

Using this criterion for $n=2$ and $n=3$, we find that, for $n=2$, all of our events are classified as either $\Upsilon\to\gamma\pi^+\pi^-\pi^+\pi^-$, $\Upsilon\to\gamma\pi^+\pi^-K^+K^-$, $\Upsilon\to\gamma\pi^+\pi^-p\bar{p}$, or $\Upsilon\to\gamma K^+K^-K^+K^-$. Since a true $\Upsilon\to\gamma\pi^+\pi^-\pi^+\pi^-$ event will sometimes be classified as something other than an $\Upsilon\to\gamma\pi^+\pi^-\pi^+\pi^-$ event, we unfold from our observed event-type distribution the true distribution as follows: Equal numbers of Monte Carlo events of the varieties $\Upsilon\to\gamma\pi^+\pi^-\pi^+\pi^-$, $\Upsilon\to\gamma\pi^+\pi^-K^+K^-$, $\Upsilon\to\gamma\pi^+\pi^-p\bar{p}$, and $\Upsilon\to\gamma K^+K^-K^+K^-$ were used to determine a transformation matrix T_2, which provides, for each type of event generated, the likelihood of it being classified as one of the four possible event types. Thus, the matrix T_2 operates on a vector of true Monte Carlo events Y to give an observed event-type distribution vector $X=T_2Y$. By inverting this matrix, and then applying it to the observed event-type distribution X, we unfold these observed distributions to obtain the true event types.

We tabulate the signal size for each of the particle mass assumptions for the resonant data, the continuum data, and also the background from events with undetected particles (using the $|q_{\rm tot}|=1$ events) which populate the region under the signal. Subtracting the various backgrounds, we obtain the net signal size. We then apply the T_n^{-1} matrices to these observed excesses to determine the branching ratios. Results, including a summary of the transformation matrices T_n for $n=2$ and $n=3$,[14] are given in Tables I–III. Also presented are the branching ratios as predicted by the tuned LUND Monte Carlo simulation of $\Upsilon(1S)\to gg\gamma$. The Monte Carlo prediction is in general agreement with our measurements. The systematic errors which we present are due to several sources: our uncertainty in photon finding efficiency, our uncertainty in the photon position resolution, our uncertainty in the dE/dx calibration used to identify particles (which affects the number of particle-type permutations we consider as candidates), and our uncertainty in modeling the particle momentum distributions.

The $n=2$ data sample was also examined for the possibility that the final-state hadrons were being produced through some intermediate state (either ρ^0, K^*, Δ, or ϕ). Figure 6 shows the $M(h^+h^-)$ vs $M(h^-h^+)$ (h here represents either a pion, kaon, or proton) invariant-mass scatter plots, as well as their projections onto one axis. No obvious substructure is observed in the $\pi^+\pi^-$, $p\pi^-$, or K^+K^- invariant-mass plots; however, we notice an apparent clustering of events in the $\Upsilon\to\gamma\pi^+\pi^-K^+K^-$

event sample which suggests $\Upsilon(1S)\to\gamma K^{*0}\bar{K}^{*0}$. In particular, we find 7.4 ± 3.3 events[15] which fit this hypothesis in our $\Upsilon(1S)$ data sample. No such clustering is observed in the continuum data set. The intermediate state $\Upsilon(1S)\to\gamma K^{*0}\bar{K}^{*0}$ therefore accounts for $(26\pm11)\%$ of our observed $\Upsilon\to\gamma\pi^+\pi^-K^+K^-$ decay rate.

Results from $\psi(3097)$ decays have shown that a large number of radiative decays proceed through exclusive two-body processes. We have therefore searched for resonant structure in the recoil hadronic system opposite the photon in our data set, using a technique independent of the mass of the daughter particles. For the two-body decay $\Upsilon\to\gamma X$, the mass of the recoil hadronic state X is related to its momentum p_h by the relation

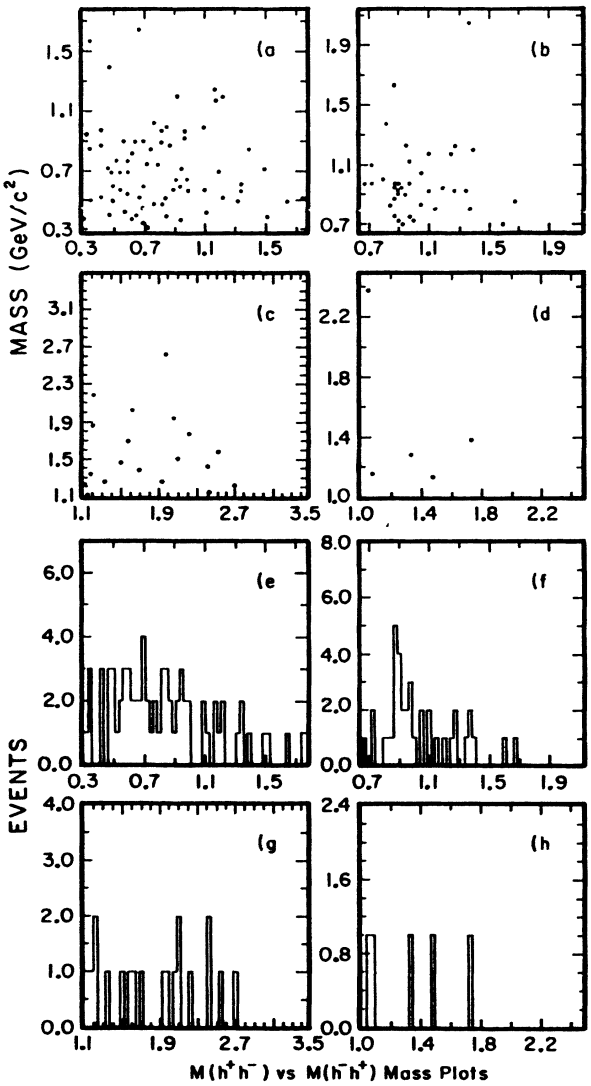

FIG. 6. $n=2$ submass $M(h^+h^-)$ vs $M(h^-h^+)$ scatter plots and projections onto x axis. (a) $M(\pi^+\pi^-)$ vs $M(\pi^-\pi^+)$ and (e) projection of plot (a) onto x axis; (b) $M(K^+\pi^-)$ vs $M(K^-\pi^+)$ and (f) projection of plot (b) onto x axis; (c) $M(p^+\pi^-)$ vs $M(p^-\pi^+)$ and (g) projection of plot (c) onto x axis. (d) $M(K^+K^-)$ vs $M(K^-K^+)$ and (h) projection of plot (d) onto x axis.

$$M_X=[(M_\Upsilon-p_h)^2-p_h^2]^{1/2}\ .$$

In Fig. 7, we present the recoil mass calculated for the $n=2$ and $n=3$ cases, in which the bin width corresponds to one unit of resolution in this quantity. Plotted vertically is the implied $\Upsilon(1S)$ branching ratio. No structure is observed.[16]

We have also conducted dedicated searches for the $\eta(1430)$ (formerly ι) and the $f_2(1720)$ (formerly θ). The $\eta(1430)$ is observed in radiative ψ decay with a relatively large product branching ratio: $B(\psi\to\gamma\eta;\eta\to K\bar{K}\pi)=(0.47\pm0.06)\%$. We look for it in the final state $K_S^0K^\pm\pi^\mp$, where the K_S^0 is detected as a charged-track pair forming a "vee" displaced from the interaction point. We do not find any candidate events and set a 90% confidence level upper limit of 8.2×10^{-5} on the branching ratio for this decay chain, corresponding to a suppression of approximately 50 relative to the rate observed from the ψ for this mode.

The $f_2(1720)$ was searched for through the decay chain $\Upsilon(1S)\to\gamma f_2$, $f_2\to K_S^0K_S^0$. We find one event consistent with a $\gamma K_S^0K_S^0$ topology and measure the invariant mass of the $K_S^0K_S^0$ system to be 2.674 GeV/c^2. No events are observed at the f_2 mass, yielding an upper limit of 3.6×10^{-4} on this decay mode.

IV. ANALYSIS AND RESULTS: $\Upsilon\to\gamma n(h^+h^-)$, $n=1$

Two charged-track events which satisfy the event-selection requirements of Sec. II are, in addition, subjected to a kinematic fit, imposing overall energy-momentum conservation under the three possible hadron-type assumptions. We retain events with $\chi^2<30$ (Ref. 17) and calculate the invariant mass of the recoil hadrons.

This invariant mass is plotted in Fig. 8, calculated under the assumption that the recoil tracks are pions, sepa-

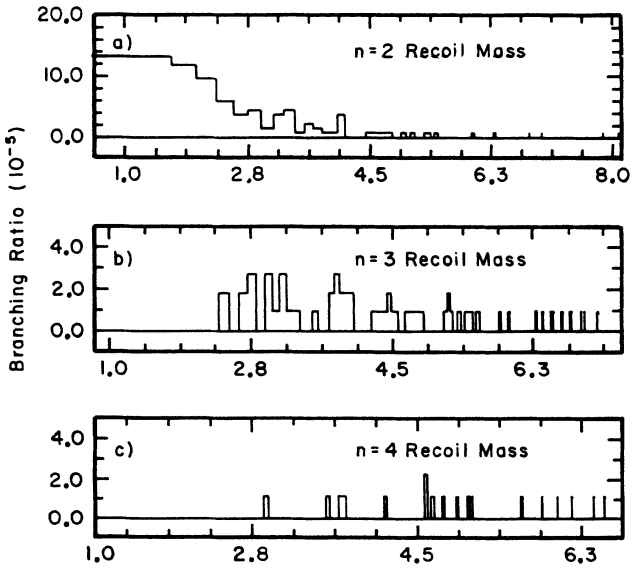

FIG. 7. Mass distribution recoiling against photon.

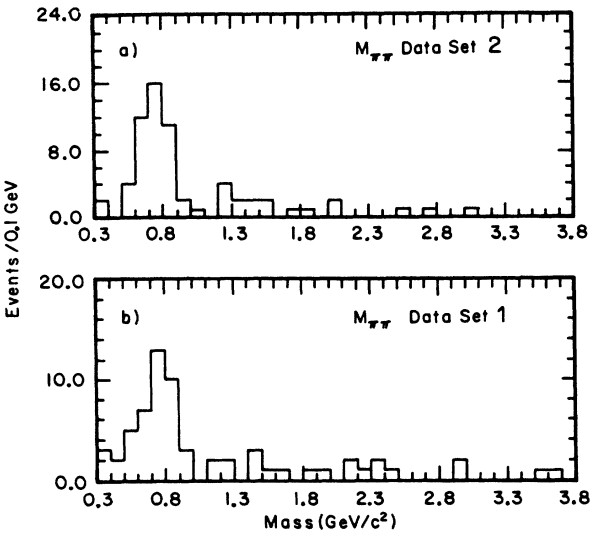

FIG. 8. Dipion invariant mass for radiative two-track $\Upsilon(1S)$ decays.

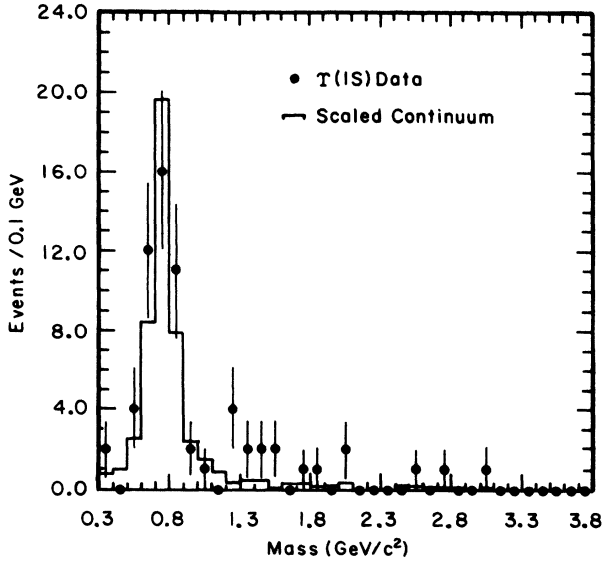

FIG. 9. $n=1$ invariant-mass plots for continuum events satisfying kinematic fit criteria with $\Upsilon(1S)$ data overplotted.

rately for the data set 1 and data set 2 samples. Owing to the enhanced electron identification in the data sample 2, we expect the radiative Bhabha rejection in this sample to be more efficient than in the sample 1. We therefore only use the data sample 2 in the calculation of our final branching ratios and upper limits. We note that our present result from data set 1 disagrees with our previously published result[18] using the same data set. In the previous analysis, we had attempted to reduce the radiative Bhabha background by rejecting events with large shower energy or too many unmatched showers. However, we underestimated the effects of noise and nuclear interactions of charged pions in the calorimeter, and therefore rejected a large number of real $e^+e^-\to\gamma\pi^+\pi^-$ events. The upper limits presented in the original publication are therefore too low.

Prominent in both these invariant-mass plots is the presence of a large ρ^0 signal, as is expected theoretically and verified experimentally[6] by other analyses. This is consistent with our expectation that backgrounds due to QED processes (particularly $e^+e^-\to q\bar{q}\gamma$, where the $q\bar{q}$ system has an invariant mass in the ρ region) are expected to be quite large. We have checked this background by performing an identical analysis on our continuum data sample to determine the continuum contribution to our $\Upsilon(1S)$ signal. The scaled continuum data are shown in Fig. 9 with the data collected at the $\Upsilon(1S)$ resonance overplotted. The agreement is good, indicating that, within errors, the $\gamma\rho^0$ rate is wholly accounted for by continuum production. We use our $\Upsilon(1S)$ data to calculate an effective observed cross section over the solid angle covered by $0.56\geq|\cos\theta|$ (Ref. 19): $\sigma(e^+e^-\to\rho^0\gamma)=(3.12\pm0.61)\times10^{-3}$ nb. This is in agreement with the analysis by the ARGUS Collaboration.[6] It is substantially higher than the upper limits for this process reported by the CUSB Collaboration in an analysis of the inclusive photon spectrum near the end point which they used to set limits on two-body radiative decays of the $\Upsilon(1S)$ into a photon plus low-mass hadronic states.[20]

Although the decay $\Upsilon(1S)\to\rho^0\gamma$ is prohibited by charge conjugation, the hadronic decay $\Upsilon(1S)\to\rho^0\pi^0$ is allowed. In the case where the two photons emerge sufficiently close to one another that they produce showers which merge in the outer calorimeter, the decay $\Upsilon(1S)\to\rho^0\pi^0$ will produce the same observed topology as $\Upsilon(1S)\to\rho^0\gamma$. It is therefore possible that some of the ρ^0 events which we observe arise from such $\Upsilon(1S)$ hadronic decays. We have checked this possibility in a direct search for the decay $\Upsilon(1S)\to\rho^0\pi^0$. Since our calorimeter

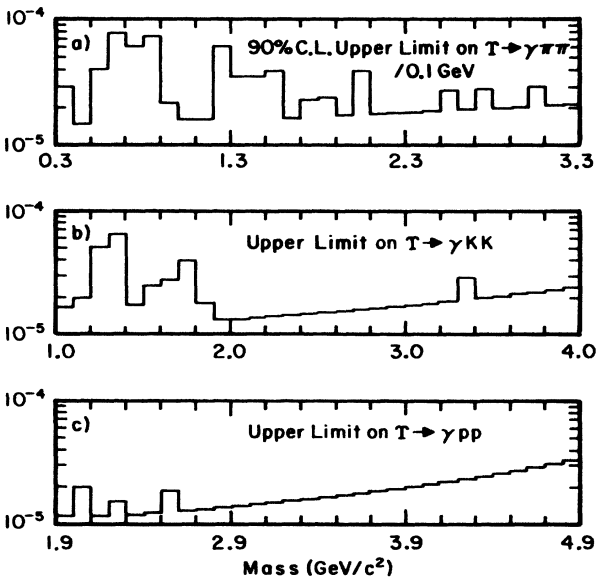

FIG. 10. Upper limits on $\Upsilon(1S)\to\gamma X$, $X\to h^+h^-$.

TABLE IV. Summary of $\Upsilon \to \gamma(h^+h^-)$ 90%-C.L. upper limits.

Reaction	Prediction (Ref. 2)	Upper limit
$B(\Upsilon(1S)\to\gamma f_2(1270))B(f_2(1270)\to\pi^\pm\pi^\mp)$	$\approx 7\times10^{-5}$	1.2×10^{-4}
$B(\Upsilon(1S)\to\gamma f_2'(1525))B(f_2'(1525)\to K^\pm K^\mp)$	$\approx 2\times10^{-5}$	5×10^{-5}
$B(\Upsilon\to\gamma\eta(1430))B(\eta\to K^\pm\pi^\mp K_S^0)$		8.2×10^{-5}
$B(\Upsilon(1S)\to\gamma f_2(1720))B(f_2(1720)\to K_S^0K_S^0)$		3.6×10^{-4}
$B(\Upsilon(1S)\to\gamma f_2(1720))B(f_2(1720)\to K^\pm K^\mp)$		1.2×10^{-4}

is located 2.5 m from the interaction point, and the spatial resolution for the position resolution of showers is of order 2 cm, the angular resolution is quite good; for a π^0 of energy 4.5 GeV, the two photons should remain distinct 35% of the time. We find no events consistent with our hypothesized decay, and, given a detection efficiency of 4% (including the efficiency for resolving the photons), we set an upper limit of 6.6×10^{-5} (90% confidence level) for this branching ratio based on this direct search.

The efficiency for detecting $\Upsilon\to\gamma(h^+h^-)$ candidate events is determined with the use of Monte Carlo simulations. For low-mass objects, where the two tracks tend to emerge very close to one another, the event detection efficiency is primarily limited by the geometrical acceptance of the barrel calorimeter. For higher-mass objects, the efficiency decreases since the two tracks are less likely to both point towards the fiducial volume of the detector; in addition, as the hadronic recoil mass increases, the photon energy diminishes. Below a photon energy of 2 GeV, the trigger efficiency, largely based on the total pulse height in the calorimeter, begins to drop. The overall detection efficiency is well approximated by a linearly decreasing function of recoil mass, starting at approximately 40% for recoil masses at threshold, and dropping to close to zero for recoil masses 5 GeV/c^2 above threshold.

After performing a continuum subtraction, no obvious structure is observed in the recoil mass plot. Limits on branching ratios for exclusive radiative decays of the $\Upsilon(1S)$ into a photon plus another particle decaying into two charged tracks are presented in Fig. 10 for the three-particle species, and are consistent with other analyses.[6,21] The only region of the invariant-mass plot suggestive of an excess above the continuum appears in the region $m_{\pi\pi}=1.4$ GeV/c^2; where we count ten events in the interval 1.2 GeV$<m_{\pi\pi}<$1.6 GeV/c^2; the background in the same region corresponds to two events. However, there is no radiative decay of the ψ which produces a corresponding resonance in this mass region. Comparison of our results with theoretical predictions is presented in Table IV.[22]

V. SUMMARY

In summary, we have observed exclusive radiative decays of the $\Upsilon(1S)$ meson in decay modes into a photon plus four, six, or eight charged tracks. Topological branching ratios are consistent with those predicted by the LUND Monte Carlo simulation of the process $\Upsilon(1S)\to gg\gamma$. Despite difficulties in ascertaining definite final states, we have observed positive evidence for the production of baryons in exclusive radiative decays. An analysis of the $\Upsilon\to\gamma\pi^+\pi^-K^+K^-$ mode indicates that roughly one-quarter of these decays are proceeding through the mode $\Upsilon(1S)\to\gamma K^{*0}\bar{K}^{*0}$. For the decay $\Upsilon\to\gamma(h^+h^-)$, no structure is observed in the recoil hadron mass, and upper limits are set which are on the order of theoretical predictions.

ACKNOWLEDGMENTS

We are grateful for the indefatigable efforts of the entire CESR staff which made this work possible. The work was supported by the National Science Foundation and the U.S. Department of Energy under Contracts Nos. DE-AC02-76ER01428, DE-AC02-76ER03064, DE-AC02-76ER01545, DE-AC02-78ER05001, DE-AC02-83ER40105, and DE-FG05-86ER40272. The Cornell National Supercomputing Facility, funded in part by the NSF, New York State, and IBM, was used in this research. P.S. Drell thanks the Presidential Young Investigator Program of the NSF, R. Kass thanks the Office of Junior Investigator program of the DOE, and R. Poling thanks the Sloan Foundation for their support.

[1]Particle Data Group, G. P. Yost *et al.*, Phys. Lett. B **204**, 1 (1988).
[2]J. G. Körner *et al.*, Nucl. Phys. **B229**, 47 (1983).
[3]D. Andrews *et al.*, Nucl. Instrum. Methods **A211**, 47 (1983).
[4]D. G. Cassel *et al.*, Nucl. Instrum. Methods **A252**, 325 (1986).
[5]Robert W. Kowaleski, Ph.D. thesis, Cornell University, 1988.
[6]H. Albrecht *et al.*, Z. Phys. C **42**, 349 (1989).
[7]F. A. Berends and R. Kleiss, Nucl. Phys. **B177**, 237 (1986).
[8]The "energy-weighted" spread of the shower is the rms width of the hits in the electromagnetic calorimeter corresponding to a shower, with each hit weighted by the pulse height at that coordinate.
[9]We compare with the $n=2$ sample; for higher multiplicities the average photon energy lies below the value for which π^0 merging occurs.
[10]T. Sjøstrand and M. Bergstrom, Comput. Phys. Commun. **43**, 367 (1987); T. Sjøstrand, *ibid.* **39**, 347 (1986).
[11]David Z. Besson, Ph.D. thesis, Rutgers University, 1986.
[12]R. L. Ford and W. R. Nelson, SLAC Report No. SLAC-210 (unpublished).

[13]CLEO Collaboration, S. E. Csorna *et al.*, Phys. Rev. Lett. **36**, 1222 (1986); ARGUS Collaboration, H. Albrecht *et al.*, Phys. Lett. B **199**, 292 (1987); Crystal Ball Collaboration, J. Schutte *et al.*, DESY Report No. 89-007, 1989 (unpublished).

[14]For $n=3$, we find that the observed events are predominantly four- or six-pion events; correspondingly, we limit ourselves to such cases when constructing T_3. We find two events consistent with $\Upsilon(1S)\to\pi^{\pm}\pi^{\mp}K_S^0K_S^0$, where the K_S^0 is detected in the $\pi^{\pm}\pi^{\mp}$ decay mode. Our six-pion number does not include these two events.

[15]We obtain this value after performing a subtraction of the background due to $\Upsilon(1S)\to K^{*0}\pi^+K^-$, where the π^+K^- do not derive from a parent $\bar{K}^{*0}$ and have an invariant mass which happens to fall in the $\bar{K}^{*0}$ mass region. This is done using mass combinations in the $\bar{K}^{*0}$ sidebands. The errors presented here are statistical only.

[16]As is appropriate for the decay of the $\Upsilon(1S)$ into a photon plus a pseudoscalar, a pseudoscalar recoil particle should be produced with an angular distribution of $1+\cos^2\theta$ with respect to the beam axis. For such a case, since our acceptance favors $|\cos\theta|=0$, the corresponding branching ratio values presented here would be degraded by approximately 30%.

[17]Monte Carlo studies indicate that this cut is virtually 100% efficient; the Monte Carlo error distributions have been checked and show good agreement with $\mu^+\mu^-\gamma$ events obtained from data.

[18]CLEO Collaboration, A. Bean *et al.*, Phys. Rev. D **34**, 905 (1986).

[19]The fact that our fiducial acceptance is 47% and not 56% results from the presence of dead space in ϕ in our detector. Our "observed" cross section thus assumes that there is no angular dependence on ϕ in the cross section $dN(\rho\gamma)/d(\phi)$; the quoted results have been correspondingly efficiency corrected for the geometric acceptance in ϕ.

[20]J. Lee Franzini, in *Proceedings of the XXIV International Conference on High Energy Physics,* Munich, West Germany, 1988, edited by R. Kotthaus and J. H. Kühn (Springer, Berlin, 1989).

[21]S. E. Baru *et al.*, Z. Phys. C **42**, 505 (1988).

[22]These upper limits are obtained by performing fits to the data using the Particle Data Group values for the masses and widths of the indicated states.